Faculty of Natural and Applied Sciences Journal of Scientific Innovations
Print ISSN: 2814-0877 e-ISSN: 2814-0923
www.fnasjournals.com
Volume 6; Issue 3; May 2025; Page No. 15-27.
DOI: https://doi.org/10.63561/fnas-jsi.v6i3.946

Corrosion Inhibition and Dye Studies of Mixed-Ligand Metal (II) Complexes: Synthesis and Characterisation

***Iyo, I.A., Festus, C., &Amadi, J.U.**
Department of Chemistry, Ignatius Ajuru University of Education, Rivers State, Nigeria

***Corresponding author email:** atekeari267@gmail.com

Abstract
A new series of imine ligands and their M(II) complexes were synthesized via reflux from the aldol condensation of 2-hydroxy-1-naphthaldehyde and precursor **4** ($C_8H_8N_2S$) and **6** ($C_5H_7N_3O$) respectively. The FT-IR results showed ranges between 1667–1678cm^{-1} for the ligands and 1618–1658cm^{-1} for the M(II) complexes, indicating the formation of the azomethine group, and the coordination of the M(II) ions to the azomethine during complexation, hence, the longer band stretches. The bands 506–525cm^{-1} and 410–450cm^{-1} present in the M(II) complexes only, indicated M-O and M-N linkages, respectively. The UV-Vis bands 30960–50000 cm^{-1} and 26667–32467 cm^{-1} respectively indicated the presence of $\pi \rightarrow \pi^*$ and $n \rightarrow \pi^*$ of cyclic ring in the ligands and M(II) complexes. The solubility and thermal decomposition results showed that all compounds were insoluble in distilled H_2O and were thermally stable at room temperature. At 303K the corrosion inhibition efficiency ranges 24.03–91.28% for the ligands, 60.92–98.65% for the metals, and at 373K the ranges 11.68–71.68% for the ligands, and 33.67–98.07% for the metals, showed that all the imine compounds possessed corrosion inhibition efficiencies governed by concentration, time and temperature, with the M(II) complexes showing better corrosion inhibition efficiencies. All imine compounds viably showed very-good to excellent dye properties on both natural and synthetic fabrics of wool, cotton, goat-hair and nylon, with color-fastness range 4–5 on the Standard Blue Scale. Hence, the imine compounds, possessing significant dyeing properties, are excellent alternative dyeing agents on textile fabrics.

Keywords: Imine Ligand, M(II) Complexes, Mild Steel, Corrosion Inhibition, Dye.

Introduction

Imines are known to have special applications in many sectors of applied scientific knowledge, including medicine, industry, agriculture, chemistry and biochemistry (Yang et al., 2016). They play a special role as chelating ligands in both main group and transition metals, giving rise to several interesting applications and uses (Goff & Ouazzani, 2014). Imine derived from acid hydrazide and aldehyde or ketone, for example, has been known to exhibit potential poly-nucleating behavior, coordinating through azomethine nitrogen, ketonic/enolate oxygen, and phenolate oxygen, thus, offering a variety of bonding possibilities in several metal complexes formed with it. This imine has also drawn keen interest to researchers in recent years following its potency of wide variety of biological and pharmaceutical properties. (Mohanraj et al., 2016).

The application of science and technology has greatly enhanced life and advanced the frontiers of development. Many technological outfits, including industries, construction materials, machines and many other engineering materials and equipment, have contributed enormously to the advancement of life. Yet, corrosion has been a major plague truncating the advancement of these technological outfits (Festus et al., 2023). Burak & Mehmet in Festus et al., (2023) asserted that corrosion consequences are serious and have become a global concern. The impacts or consequences of corrosion are not just commercial. Some of the negative impacts include contamination of product, growth truncation and cessation of plant, wastage of treasured resources, low efficiency of equipment and product performance, expensive repairs and maintenance, and exclusive overdesign (Festus et al., 2023).

One promising and viable way to inhibit corrosion of metal frameworks whose application is inevitably found in corrosion-initiating milieu is the use of imines. These organic frameworks (imines) serve as a good option following

Cite this article as:
Iyo, I.A., Festus, C., &Amadi, J.U. (2025). Corrosion inhibition and dye studies of mixed-ligand metal (II) complexes: synthesis and characterization. *FNAS Journal of Scientific Innovations*, *6*(3), 15-27. https://doi.org/10.63561/fnas-jsi.v6i3.946

their relative economic affordability, ecological friendliness and enhanced usability, as compared to conventional methods of corrosion inhibition (Festus et al., 2023).

For the unique functions of imine ligands and their M(II) complexes many transition metal complexes from this kind of imines have been synthesized, such as, Al(III), Fe(III), Cot(II), Ni(II) and Cu(II) complexes (Festus et al., 2021). These M(II) ions and others have been used as mordant in dyeing techniques, with the hydroxyl-substituted imines and their metal complexes being shown to have the hydroxyl group and the metal ion group engaging in the bonding process, thus, facilitating the action required for the purpose of staining or dyeing (Yang et al., 2016). The difference in the location and properties of the hydroxyl groups might give this imines advantages to be remarkable good agents for the assigned purposes (Abuamer et al., 2014).

Materials and Methods

All analytical grade reagents/chemicals ($C_{11}H_8O_2$ and precursors **4** (A-4-MBTZ) and **6** (A-4-A-6-MP), $FeSO_4.7H_2O$, $(CH_3COO)_2Cu.H_2O$, $(CH_3COO)_2Zn.2H_2O$, $NiCl_2.6H_2O$; $(CH_3)_2SO$, C_3H_7NO, CH_2Cl_2, and $CHCl_3$) were supplied by Sigma-Aldrich Company Limited and used as obtained. The Fourier Transform Infrared (FT-IR) spectra were recorded on Thermo Nicolet Avater 370, while Shimadzu UV-160A spectrophotometer was utilized to obtain the electronic (UV–Vis) data.

Synthesis of L2H and L1H Imine ligands

A procedure similar to that documented in literature by Festus et al. (2023) was adopted in the syntheses of the ligands (L1H) and (L2H). The latter were synthesized using 8 g (0.046 5 mol) of 2-hydroxynaphthaldehyde to react with equimolar mass of **4**, and **6** respectively. These were mixed in hot 50 mL acidified absolute ethanol in a quick-fit condenser apparatus and refluxed at a carefully regulated temperature range for 6h. After refluxing the orange and yellow precipitate respectively was filtered using Buchner filtration apparatus, recrystallized in hot absolute ethanol and left for 24h to air-dry. The measured weights of L1H and L2H were 6.310g (42.655%) and 5.247g (40.43%) respectively.

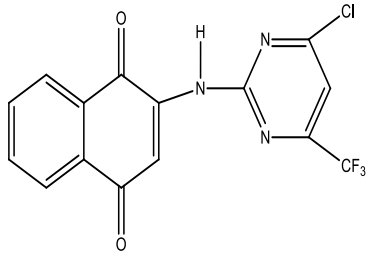

2-((4-chloro-6-(trifluoromethyl)pyrimidin-2-yl) amino)naphthalene-1,4-dione

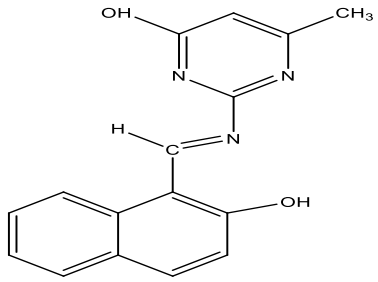

(*E*)-2-(((2-hydroxynaphthalen-1-yl)methylene) amino)-6-methylpyrimidin-4-ol

Cite this article as:
Iyo, I.A., Festus, C., &Amadi, J.U. (2025). Corrosion inhibition and dye studies of mixed-ligand metal (II) complexes: synthesis and characterization. *FNAS Journal of Scientific Innovations*, *6*(3), 15-27. https://doi.org/10.63561/fnas-jsi.v6i3.946

Fig.1: Ligand L1H (2L7B)

Fig.2: Ligand L2H (2L8A)

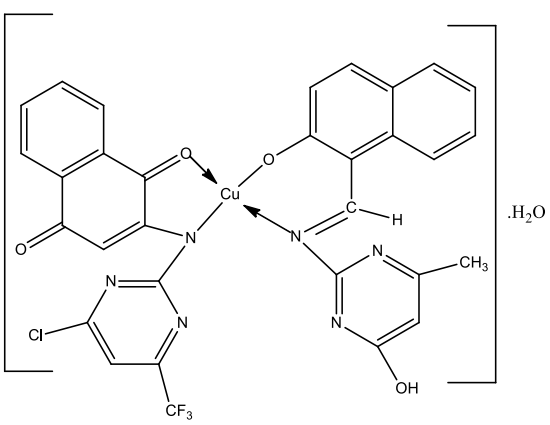

(*E*)-((4-chloro-6-(trifluoromethyl)pyrimidin-2-yl)(1,4-dioxo-1,4-dihydronaphthalen-2-yl)amino)((1-(((4-hydroxy-6-methylpyrimidin-2-yl) imino)methyl)naphthalen-2-yl)oxy)copper hydrate

Fig.**3**: **[Cu(L_1)(L_2)].H_2O**

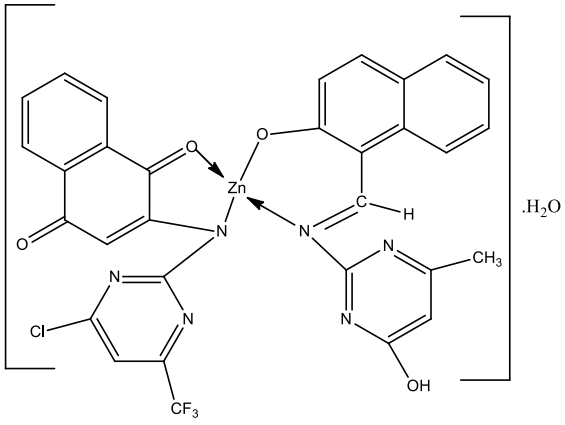

(*E*)-((4-chloro-6-(trifluoromethyl)pyrimidin-2-yl)(1,4-dioxo-1,4-dihydronaphthalen-2-yl)amino)((1-(((4-hydroxy-6-methylpyrimidin-2-yl) imino)methyl)naphthalen-2-yl)oxy)zinc hydrate

Fig.**4**: **[Zn(L_1)(L_2)].H_2O**

Synthesis of M(II)-L1H/L2H complexes

A procedure similar to that already in Festus et al. (2022) was adopted in the synthesis of each of the M(II) complexes (Figures 3-6). 0.800g of (L1H) was used to calculate equimolar mass of L2H (0.701g), $FeSO_4.7H_2O$ (0.7006g), $(CH_3COO)_2Cu.H_2O$ (0.503g), $(CH_3COO)_2Zn.2H_2O$ (0.553g), $NiCl_2.6H_2O$ (0.599g). The measured mass of the metal salt and the ligands were mixed in hot 50mL absolute ethanol catalyzed with a few drops of acid in a quick-fit condenser apparatus and refluxed at a carefully regulated temperature range of 55–65℃ for 6h. After refluxing, the precipitate was filtered and the dried M(II) mixed ligand complex was isolated.

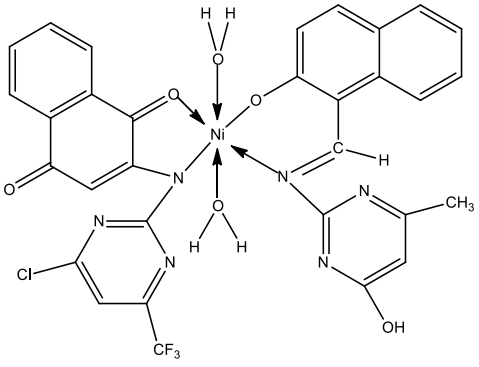

(*E*)-((4-chloro-6-(trifluoromethyl)pyrimidin-2-yl)(1,4-dioxo-1,4-dihydronaphthalen-2-yl)amino)((1-(((4-hydroxy-6-methylpyrimidin-2-yl)imino)methyl)naphthalen-2-yl)oxy)nickel dihydrate

Fig.**5**: **[Ni(L_1)(L_2)(H_2O)$_2$]**

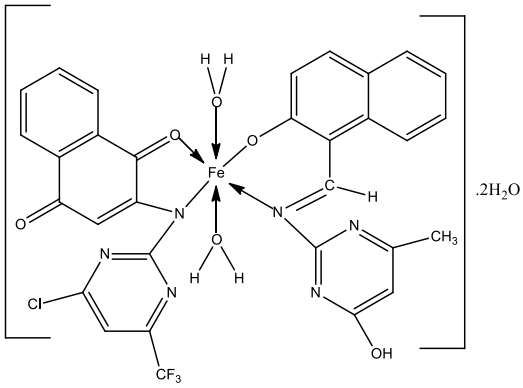

(*E*)-((4-chloro-6-(trifluoromethyl)pyrimidin-2-yl)(1,4-dioxo-1,4-dihydronaphthalen-2-yl)amino)((1-(((4-hydroxy-6-methylpyrimidin-2-yl)imino)methyl)naphthalen-2-yl)oxy)iron dihydrate

Fig.**6**: **[Fe(L_1)(L_2)(H_2O)$_2$].2H_2O**

The dye procedure

The dye procedure was carried out in line with that recorded in Abuamer et al. (2018). Yam fibers of wool, cotton, nylon and goat-hair were cut in dimensions. Each yam fiber was tested, without mordant, for colour-fastness and colour-bleeding by preparing respective solutions of each ligand and each M(II) complex in 1L beaker, and soaking each fiber into the ligand and M(II) complex solutions. Afterward, each soaked fiber was air-dried and washed in soapy H_2O and rinsed in clean H_2O, respectively, and the colour-fastness recorded on a grade of 1–5 (1 = poor, 5 = excellent) using the Standard Blue Scale, at a temperature of 40℃.

Cite this article as:
Iyo, I.A., Festus, C., &Amadi, J.U. (2025). Corrosion inhibition and dye studies of mixed-ligand metal (II) complexes: synthesis and characterization. *FNAS Journal of Scientific Innovations*, *6*(3), 15-27. https://doi.org/10.63561/fnas-jsi.v6i3.946

Gravimetric measurements and preparation of ms coupons

As with the procedure in Festus et al. (2022), about 87mL of HCl was measured out from the AR reagent bottle into a 1000mL volumetric flask to make a 1M acid solution and made to sufficient quantities enough for all corrosion studies. Different concentrations of 15 ppm, 30 ppm and 60 ppm for each ligand and M(II) complex were prepared in sufficient quantities needed for the weight loss (WL) experiment, and each weight loss done in threefold, and the average determined. All corrosion experiment was carried out in 5 h in a thermostat H_2O-bath, at 30℃ and 100℃ respectively, for each concentration of each imine ligand and each M(II) complex in a 50 mL beaker containing the 1M HCl acid solution and the respective concentration of the inhibitor. Sufficient ms coupons were cut into $2\ cm \times 2\ cm \times 0.075\ cm$, abraded with emery paper to de-rust the ms surface, then after, washed with soapy H_2O, rinsed in distilled H_2O, degreased in absolute ethanol and immersed briefly in acetone and left in moisture-free place to dry. The dry ms coupons were weighed and immersed in each 50mL beaker containing the respective concentration of solution of each ligand and M(II) complex respectively in 1M HCl solution. After 5 h for each temperature of 30℃ and 100℃, respectively, the ms coupons were re-polished with emery paper, re-washed and re-rinsed in distilled H_2O, re-degreased in ethanol and re-immersed briefly in acetone, left to dry and re-weighed. The weight loss (Δw), corrosion rate (CR) and Inhibition efficiency (IE) were calculated, according to Festus & Wodi (2021), using the respective equation:

$$\Delta w = \frac{m_1 - m_2}{A} \ldots\ldots\ldots\ldots\ldots\ldots\ldots\ldots 1$$

Where, $m_1 =$ initial weight, and $m_2 =$ final weight, and A = surface area of coupon.

$$CR = \frac{\Delta w}{DAT} \ldots\ldots\ldots\ldots\ldots\ldots\ldots\ldots 2$$

Where D, and T are density and time, respectively; and $IE = \left(\frac{\Delta w}{m_1}\right) \times 100 \ldots\ldots\ldots\ldots\ldots\ldots\ldots 3$

Results

Table 1: Analytical data for synthesized imine ligands and M(II) complexes

Ligand/ complex	Melting point (℃)	Colour	Molecular formula	MW (gmol^{-1})	% yield
L2H	179 – 182	Pale yellow	$C_{16}H_{13}O_2N_3$	279.2993	40.43%
L1H	174 – 178	Orange	$C_{19}H_{14}ON_2S$	318.399	42.65%
[Fe(L1)(/L2)$(H_2O)_2$].2H_2O	180 – 185	Pale yellow	$FeC_{35}H_{26}O_3N_5S.2H_2O$	688.566	32.34%
Cu – L_1/ L_2	193 – 195	Deep brown	$CuC_{35}H_{26}O_3N_5S.\ 2H_2O$	696.237	40.70%
[Zn(L1)(/L2)].H_2O	250 – 255	Orange	$ZnC_{35}H_{26}O_3N_5S.\ 2H_2O$	698.101	16.1%
[Ni(L1)(/L2)$(H_2O)_2$]	200 – 207	Pale green	$NiC_{35}H_{26}O_3N_5S.\ 2H_2O$	691.414	13.7%

Table 2: UV-Vis spectroscopic data for the imines and their M(II)complexes

Compounds	Absorption (cm^{-1})	Band assignment
L2H	32051	$\pi \rightarrow \pi^*$
	26667; 27302; 28409	$n \rightarrow \pi^*$
L1H	30960	$\pi \rightarrow \pi^*$
	27322	$n \rightarrow \pi^*$
[Fe(L1)(/L2)(H2O)$_2$].2H_2O	47170	$\pi \rightarrow \pi^*$
	32467	$n \rightarrow \pi^*$
	28090	$^3T_{1g}(F) \longrightarrow {}^3T_{2g}$
[Ni(L1)(/L2)$(H_2O)_2$]	31847	$\pi \rightarrow \pi^*$
	27701	$n \rightarrow \pi^*$
	23256	$^3A_{2g} \longrightarrow {}^3T_{2g}$
[Cu(L1)(/L2)].H_2O	31847	$\pi \rightarrow \pi^*$
	28090	$n \rightarrow \pi^*$
	27322	$^3T_{1g} \longrightarrow {}^3T_{2g}$
[Zn(L1)(/L2)].H_2O	50000	$\pi \rightarrow \pi^*$
	31250	$n \rightarrow \pi^*$
	28090	MLCT

Cite this article as:
Iyo, I.A., Festus, C., &Amadi, J.U. (2025). Corrosion inhibition and dye studies of mixed-ligand metal (II) complexes: synthesis and characterization. *FNAS Journal of Scientific Innovations*, *6*(3), 15-27. https://doi.org/10.63561/fnas-jsi.v6i3.946

Table 3: FT-IR spectral data for the ligands and their M(II) complexes

Compound(s)	v(N-H)	Phenolic v(C-O-H)/H_2O	v(=C-H)	v(C-H)	v(C=C)	v(C=N)	v(C-N)	v(C-S)	v(C-H)	v(M-O)	v(M-N)
L2H	3329	1359; 1172; 1045	3068'	2935; 2753	1619	1667	1385	-	1471	-	-
L1H	-	1319; 1147; 1035	3052; 3010	2918; 2765	1551	1921; 1678	1388	822	1463	-	-
[Fe(L1)(/L2)(H2O)$_2$] .2H$_2$O	3381	3472; 1361; 1240; 1060	3008	2984; 2762	1504	1980; 1618	1399	850	1489	506	410
[Ni(L1)(/L2)(H$_2$O)$_2$]	3328	3485; 1393; 1097	3045	2902; 2798	1538	1978; 1658	1385	836	1423	520	455
[Cu(L1)(/L2)].H$_2$O	3335	3459; 1371; 1100	3058; 3029	2922; 2752	1582	1981; 1657	1387	828	1432	525	450

Table 4: Results for dye application of the imine ligands and their M(II) complexes

Ligand/M(II) Complex	Cotton		Wool		Goat-hair		Nylon	
	non-soapy	soapy H_2O	non-soapy	soapy H_2O	non-soapy	soapy H_2O	non-soapy	soapy H_2O
L2H	5	5	5	5	5	5	4-5	4-5
L1H	5	5	5	5	5	5	4-5	4-5
[Cu(L1)(/L2)].H_2O	4-5	4-5	4-5	4-5	4-5	4-5	4-5	4
[Ni(L1)(/L2)(H_2O)$_2$]	5	5	5	5	4-5	4-5	4-5	4-5
[Zn(L1)(/L2)].H_2O	5	5	5	5	5	5	4-5	4-5
[Fe(L1)(/L2)(H_2O)$_2$].2H_2O	5	5	5	5	5	5	5	4-5

Key: 1 = poor; 2 = fair; 3 = very fair; 4 = good; 5 = excellent

Table 5: corrosion results for the* imine *compounds

Ligand/M(II) complex	Temp. (K)	Blank (Δw)	Blank (ρ)	Conc. (ppm)	Δw (g)	ρ	θ	IE (%)
L2H	**303**	0.04765	0.002345	**15**	0.0362	0.001781	0.2403	24.03
				30	0.0211	0.001038	0.5574	55.74
				60	0.0107	0.0005266	0.7754	77.54
	373	0.05515	0.002714	**15**	0.04871	0.002397	0.1168	11.68
				30	0.01722	0.0008474	0.6878	68.78
				60	0.01562	0.0007687	0.7168	71.68
L1H	**303**	0.1571	0.007731	**15**	0.0454	0.002234	0.7110	71.10
				30	0.0286	0.001398	0.8192	81.92
				60	0.0137	0.0006742	0.9128	91.28
	373	0.4146	0.0204	**15**	0.2944	0.01449	0.2897	28.97
				30	0.2323	0.01143	0.4397	43.97
				60	0.1820	0.008954	0.5611	56.1
[Zn(L1)(/L2)].H_2O	**303**	0.07675	0.003777	**15**	0.03	0.001476	0.6092	60.92
				30	0.02875	0.001415	0.6254	62.54
				60	0.01395	0.0006865	0.8182	81.82
	373	0.0866	0.004262	**15**	0.05745	0.002827	0.3367	33.67
				30	0.03231	0.001590	0.6269	62.69
				60	0.01878	0.0009242	0.7831	78.31
[Ni(L1)(/L2)(H_2O)$_2$]	**303**	0.1581	0.007780	**15**	0.0354	0.001742	0.7761	77.61
				30	0.0186	0.0009153	0.8823	88.23
				60	0.0061	0.0003002	0.96.14	96.14
	373	0.4746	0.0234	**15**	0.2544	0.01252	0.4650	46.50
				30	0.2021	0.009946	0.5750	57.50

Cite this article as:
Iyo, I.A., Festus, C., &Amadi, J.U. (2025). Corrosion inhibition and dye studies of mixed-ligand metal (II) complexes: synthesis and characterization. *FNAS Journal of Scientific Innovations*, *6*(3), 15-27. https://doi.org/10.63561/fnas-jsi.v6i3.946

				60	0.001944	0.0009567	0.9591	95.91
[Cu(L1)(L2)].H_2O	**303**	0.1651	0.008125	**15**	0.0245	0.001206	0.8516	85.16
				30	0.00786	0.0003868	0.9524	95.24
				60	0.002234	0.0001099	0.9865	98.65
	373	0.5647	0.02779	**15**	0.3104	0.01528	0.4502	45.02
				30	0.1120	0.005512	0.8017	80.17
				60	0.03944	0.001941	0.9301	93.01
[Fe(L1)(L2)$(H2O)_2$].$2H_2O$	**303**	0.1662	0.008179	**15**	0.0503	0.002475	0.6974	69.74
				30	0.0124	0.0006102	0.9254	92.54
				60	0.003103	0.0001540	0.9812	98.12
	373	0.4647	0.02287	**15**	0.1456	0.007165	0.6867	68.67
				30	0.1229	0.006048	0.7355	73.55
				60	0.00899	0.0004424	0.9807	98.07

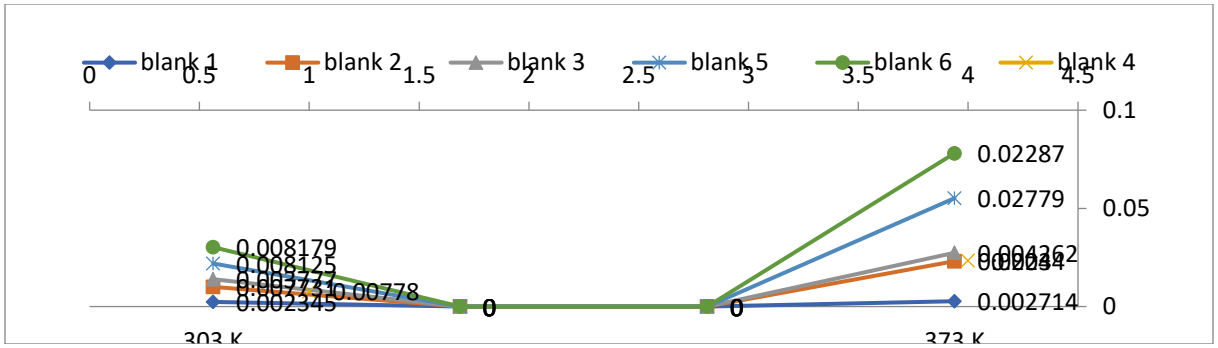

Fig. 1.: Blank for both imines and their M(II) complexes at 4 h

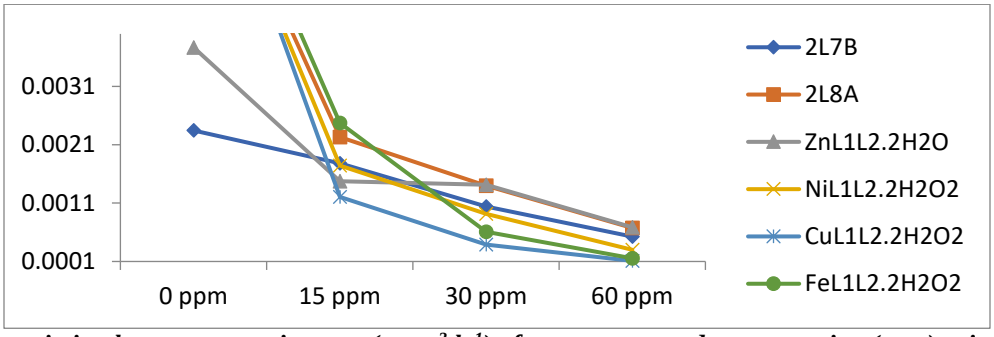

Fig. 2.: variation between corrosion rate (g cm^{-2} h^{-1}) of ms coupons and concentration (ppm) using Imine compounds at constant time of 4 h and temperature of 303K

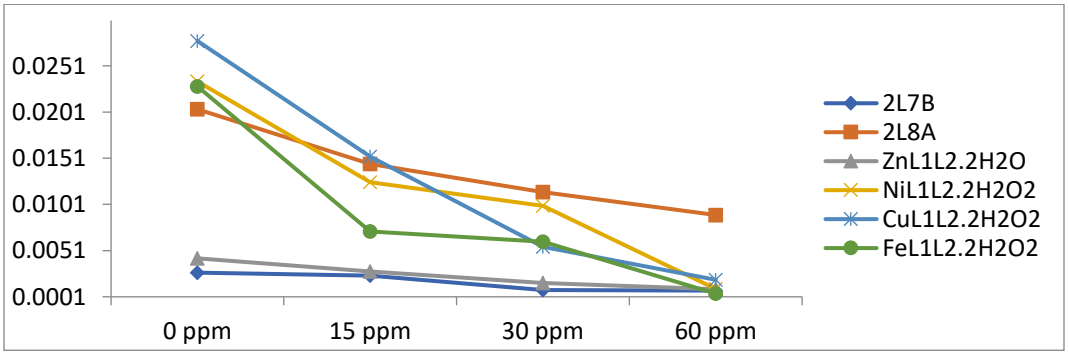

Fig. 3.: variation between corrosion rate (g cm^{-2} h^{-1}) of ms coupons and concentration (ppm) using Imine compounds at constant time of 4 h and temperature of 373 K

Cite this article as:
Iyo, I.A., Festus, C., &Amadi, J.U. (2025). Corrosion inhibition and dye studies of mixed-ligand metal (II) complexes: synthesis and characterization. *FNAS Journal of Scientific Innovations*, *6*(3), 15-27. https://doi.org/10.63561/fnas-jsi.v6i3.946

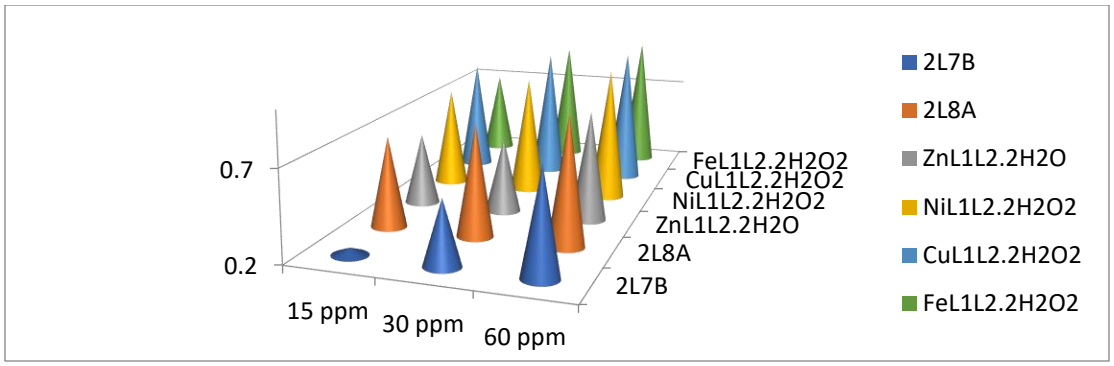

Fig. 4: variation between surface coverage of ms coupons and concentration (ppm) using imine compounds at constant time of 4 h and temperature of 303 K

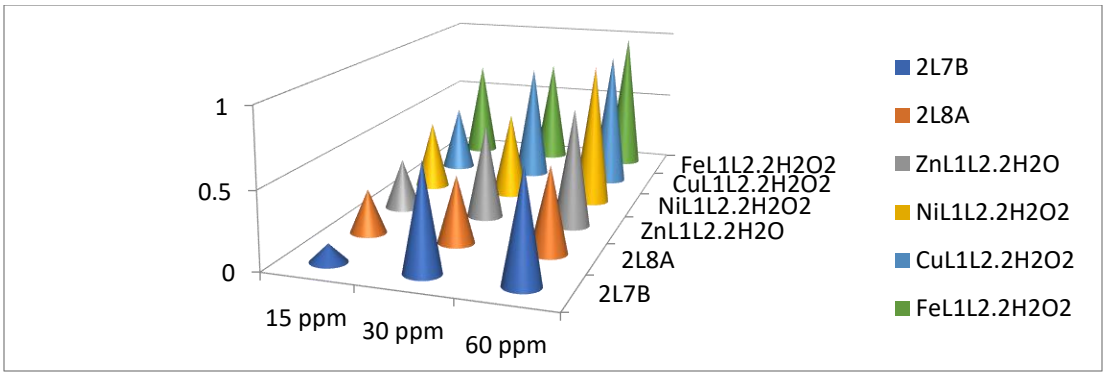

Fig. 5: variation between surface coverage of ms coupons and concentration (ppm) using imine compounds at constant time of 4 h and temperature of 373 K

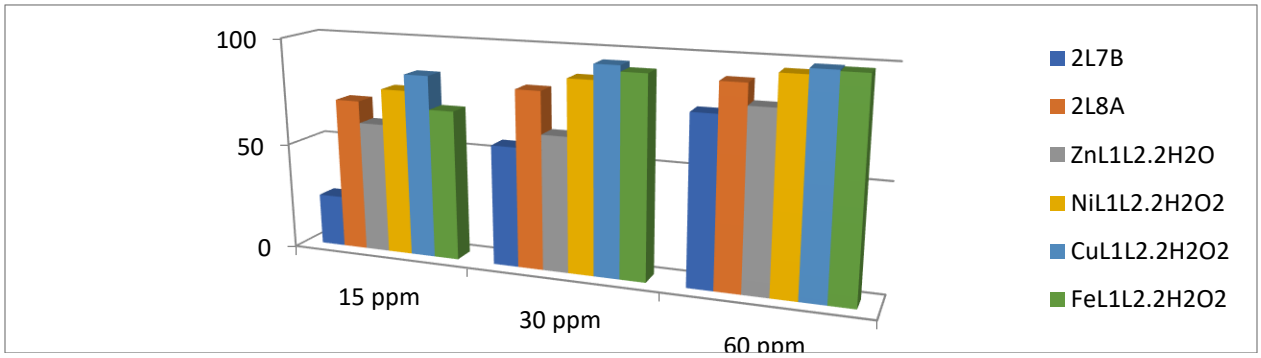

Fig. 6: variation between inhibition efficiency on ms coupons and concentration (ppm) using Imine compounds at constant time of 4 h and temperature of 303K

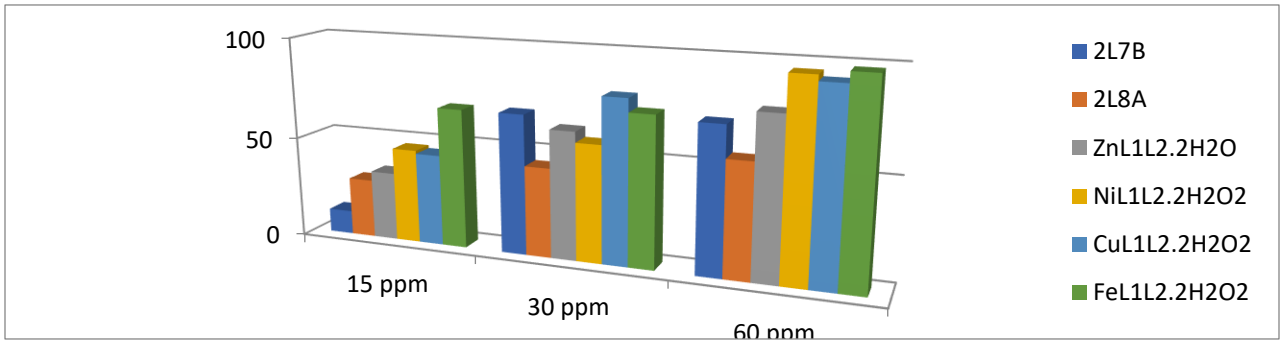

Cite this article as:
Iyo, I.A., Festus, C., &Amadi, J.U. (2025). Corrosion inhibition and dye studies of mixed-ligand metal (II) complexes: synthesis and characterization. *FNAS Journal of Scientific Innovations*, *6*(3), 15-27. https://doi.org/10.63561/fnas-jsi.v6i3.946

Fig. 7: variation between inhibition efficiency on ms coupons and concentration (ppm) using imine compounds at constant time of 4 h and temperature of 373 K

Discussion

Analytical Data

The imine ligands and their complexes had varied yields (13%-43%). Loss of product during purification or side reactions that divert reactants away from forming the desired products were some of the factors leading to a less than 100% in the yield composition. From stoichiometric point of view, the ligand reacted with the metals in 2:1 molar ratio. The imine ligands melted amid 174–182^{o}C whereas their metal complexes melted within 180–250^{o}C and above. No metal complex had the same melting point as the azomethine based chelator thereby confirming the formation of new compounds (Jane & Chioma, 2024).

Solubility data for imine ligands and their M(II) Complexes

A solubility assessment was conducted for the ligands and their M(II) complexes across seven organic solvents at room temperature. The results indicated that the compounds exhibited favorable solubility profile in C_2H_6OS, and C_3H_7NO (Jane & Chioma, 2024). Both the ligands and their divalent metal complexes showed insolubility in H_2O, suggesting their hydrophobic nature and minimal interaction with polar solvents.

Spectral studies

The UV-Vis spectroscopic results for L1H and L2H showed strong absorbance peaks at 30960cm^{-1} and 32051cm^{-1} conforming to $\pi \rightarrow \pi^*$ transitions within the ligands, arising from the benzene rings and multiple double bonds (Abel-Olaka et al., 2019; Al-qasii et al., 2023). The weak peaks at 26667cm^{-1}, 27302-27322cm^{-1} and 28409cm^{-1} indicated $n \rightarrow \pi^*$, a non-bonding to anti-bonding electronic transitions within the phenolic oxygen to carbon electron transition, and within the azomethine group, where unshared electrons transit from the lone-pair electron orbitals of the nitrogen atom to empty anti-bonding orbitals of the carbon atom (Festus et al., 2021; 2023). The metal complexes of the ligands showed noticeable shifts in absorption bands when compared to the ligands from which they were formed. For $[Fe(L1)(/L2)(H_2O)_2].2H_2O$, absorption bands of 47170cm^{-1}, 32467cm^{-1} and 28090cm^{-1} were observed. While the latter (47170cm^{-1} and 32467cm^{-1}) conformed to intra-ligand electronic transitions, the former (28090cm^{-1}) was a result of *d-d* transition $^3T_{1g}(F) \longrightarrow {}^3T_{2g}$ indicative of octahedral geometry (Abou-Hussein & Linert, 2014). The bands at 31847 cm^{-1}and 27701 cm^{-1} in $[Ni(L1)(/L2)(H_2O)_2]$ were bands assigned to the intra-ligand electron transition within the ligand moieties. These absorption bands showed noticeable bathochromic shift when compared to the imine ligand precursors of the Ni(II) complex. This observed shift in wavenumber further corroborated coordination between the donor atoms of the imine ligands and the Ni(III) ion during the synthesis. For $[Cu(L1)(/L2)].H_2O$ the absorptions bands at 31847 cm^{-1} and 28090 cm^{-1} were bands which emanated due to the intra-ligand electron transition, as established in the UV-Vis spectroscopic results of the imine ligand precursors. A closer look at these bands showed a shorter wavelength for the Cu(II) complex when compared to the imine ligand precursors. This observed shift is as a result of coordination between the oxygen,and nitrogen donor atoms of the ligands and the Cu(II) ion. The band at 27322 cm^{-1}, however, was assigned to *d-d* transition for $^3T_{1g} \longrightarrow {}^3T_{2g}$ g, suggestive of a highly distorted octahedral configuration of the Cu(II) complex, due to Jahn-Teller effect usually noticed within Cu(II) complexes (Nair et al., 2014). For $[Zn(L1)(L2)].H_2O$ the absorption bands at 50000 cm^{-1} and 31250 cm^{-1} were bands which resulted from the intra-ligand electronic transitions of the ligand moieties coordinated to the Zn(II) ion. An octahedral geometry was proposed for this complex based on its analytical conductance and spectral data. This is further supported by its diamagnetic nature and absence of d-d band, due to its complete d^{10} electronic configuration. In all the absence of bands below 10000 cm^{-1} in any of the M(II) complexes rules out entirely the possibility of a tetrahedral configuration, as, otherwise, would have been suggested for some of the M(II)complexes (Abou-Hussein & Linert, 2014).

Infrared Spectroscopy

The FT-IR results for the ligands and their M(II) complexes all showed a strong-sharp peak ranging from 1618-1678 cm^{-1}, confirmative of imine moiety presence resulting from the formation of imine ligands and their M(II)complexes (Jane & Chioma, 2024). However, the bands for the ligands were of higher wavenumber (1667 and 1678 cm^{-1} for L2H and L1H), while those for the metal complexes showed a lower wavenumber (1618 cm^{-1}, 1658 cm^{-1}, 1657 cm^{-1}) for Fe(II), Ni(II) and Cu(II) complexes respectively. The decrease in wavenumber is due to further stretching of C=N bond resulting from M-N coordination of the azomethine nitrogen atom to the M(II) ions (Jyoti & Kumar, 2019). To further corroborate the fact that there was coordination between the metal ions and the azomethine nitrogen, there was a strong sharp peak at 410 cm^{-1}, 455 cm^{-1} and 450 cm^{-1} respectively for Fe(II), Ni(II) and Cu(II) complexes. The latter (410–455 cm^{-1}) stretches were characteristic for M-N coordination (Sani & Illiyasu, 2018). The medium but sharp band at 3329 cm^{-1} for L2H distinguishes it from that of L1H (which does not have this band), indicating the presence

Cite this article as:
Iyo, I.A., Festus, C., &Amadi, J.U. (2025). Corrosion inhibition and dye studies of mixed-ligand metal (II) complexes: synthesis and characterization. *FNAS Journal of Scientific Innovations*, *6*(3), 15-27. https://doi.org/10.63561/fnas-jsi.v6i3.946

of a N-H linkage, and suggesting that nitrogen atom is part of the assemblage of L2H. The nitrogen atom as part of the cyclic assemblage in L2H at this peak is a characteristic peak for a pyrimidine moiety and suggests that L2H was likely to contain the pyrimidine moiety in its structure (Kpee et al., 2018). The sharp, strong stretch peaks at 2935 cm^{-1} (L2H), 2918 cm^{-1} (L1H); and 2984 cm^{-1} (Fe(II)), 2902 cm^{-1} (Ni(II)), and 2922 cm^{-1} (Cu(II)) complexes were characteristic of the presence of a methyl group (Festus et al., 2023). There was an accompanying stretch peak of 2753 cm^{-1} (L2H), 2765 cm^{-1} (L1H); and 2762 cm^{-1} (Fe(II)), 2798 cm^{-1} (Ni(II)), and 2752 cm^{-1} (Cu(II)) complexes, which were typical of the presence of an aldehyde C-H bonding (Memon et al., 2014), confirming that each of the ligands and their M(II) complexes were formed from their aldehyde-amine precursors in which the carbonyl group bounded with the primary amine, forming an azomethine group, and giving rise to the imine moiety. The combination of the FT-IR peaks 3000-2800 cm^{-1}, and 2800-2700 cm^{-1}, were indicative of the presence of the aldehydic moiety in the compounds. Ligand, L1H showed a strong, sharp stretch at 1385 cm^{-1} signifying cyclic (C-N) often found in the pyrimidines assemblages. The latter was also present in all other synthesized compounds with a strong-sharp signals amid 1388-1387 cm^{-1} (Festus et al., 2022). These results confirmed that L2H and L1H were bidentate having nitrogen and oxygen donor atoms available for bonding to the metal ions, thus, forming a 5-6 membered assemblage in each M(II) complexes.

Dye Results

Table 4 shows results for the dye application on the imine ligands and their M(II) complexes, without mordant and agitated for 20 min in soapy and non-soapy H_2O respectively. These results denote the degree of adsorption on the fibers of wool, cotton, goat-hair and nylon upon immersion in solution containing the dyestuff and subsequent colour-fastness test in soapy and non-soapy H_2O at the stated conditions.

There was reasonable degree of adsorption as observed for both the imine ligands and their M(II) complexes with varied results ranging from good-excellent (4-5) on a Standard Blue Scale (SBS). Hence, the ligands and their M(II) complexes showed ability of dye adsorption.

The test for colour-fastness by agitating in soapy H_2O (5 mL/100 mL) using Nittol detergent (a locally sold detergent) carried out on the cotton, wool, goat-hair and nylon fabrics of L2H showed excellent adsorption (colour-fastness), except for the nylon fabric which showed very-good result (4-5). The similar results for L2H were obtained using non-soapy H_2O – excellent for wool, cotton and goat-hair, but very-good for nylon, while L1H gave colour-fastness results due to adsorption as excellent for wool, cotton and goat-hair, but very-good for nylon. These results revealed that the imine ligands showed viable colour-fastness to the fibers for both synthetic and natural fabrics, without the use of mordant. However, colour-fastness with L2H and L1H were better on the natural fabrics (wool, cotton and goat-hair) than the synthetic fabric (nylon). This could be as a result of the structures/texture of the fabrics which were natural and hydrophilic with open cellulose structure allowing for good dye penetration, and relatively high absorbency, while the synthetic fiber nylon was hydrophobic with compact, crystalline structure and of relatively lower absorbency (Abuamer et al., 2014).

Looking at the M(II) complexes, the results for $[Cu(L1)(L2)].H_2O$ showed very-good (4-5) for all four fabrics in both soapy and non-soapy H_2O, except for the nylon fabric, which showed good result (4) for the nylon fabric in soapy H_2O. The $[Ni(L1)(L2)(H_2O)_2]$ showed excellent results (5) for both cotton and wool in soapy and non-soapy H_2O, but very-good results (4-5) for both goat-hair and nylon fabrics in soapy and non-soapy H_2O. The $[Zn(L1)(L2)].H_2O$ showed excellent results for all fabrics in both soapy and non-soapy H_2O, except for nylon, which showed very-good (4-5) result for both soapy and non-soapy H_2O. Finally, the $[Fe(L1)(L2)(H_2O)_2].2H_2O$ showed excellent results (5) for all fabrics in both soapy and non-soapy H_2O, with the exception of nylon fabric, which showed very-good result (4-5) when tested in soapy H_2O.

From all M(II) complexes, it is observed that without the use of mordant, they showed good to excellent colour-fastness to fabrics of wool, cotton, goat-hair and nylon, indicating good to excellent absorbency of the dye stuff into the fabric structures, and good to excellent adsorption of the metal-ligand donor atoms on the surface of the fabrics (Gürbüz, 2020). It has been shown that the adsorption of the metal-ligand framework of the azo-dyestuff on the fabrics was made possible through the oxygen (of the hydroxyl) and sulfur atoms of the ligand moiety, and the metal ion(s), and less or none of the azomethine group during dye adsorption, and this is most likely the situation of adsorption of these M(II) complexes on the fabric surfaces to give good to excellent colour-fastness (El-Ajaily et al., 2013). Hence, it can be concluded that the presence of oxygen, nitrogen and sulfur atoms aided the enhanced results of the ligands on the fabric surfaces.

Cite this article as:
Iyo, I.A., Festus, C., &Amadi, J.U. (2025). Corrosion inhibition and dye studies of mixed-ligand metal (II) complexes: synthesis and characterization. *FNAS Journal of Scientific Innovations*, *6*(3), 15-27. https://doi.org/10.63561/fnas-jsi.v6i3.946

Table 4 denotes that the ligands were of equal strength of colour-fastness on all. For the M(II) complexes the $[Fe(L1)(L2)(H_2O)_2].2H_2O$ showed the best result for colour-fastness, followed by $[Zn(L1)(/L2)].H_2O$, but the copper complex showed the most colour-bleeding result, especially when tested in the soapy H_2O for the nylon fabric. However, all ligands and their M(II) complexes did not show excellent colour-fastness on the nylon fabric, apart from the $[Fe(L1)(L2)(H_2O)_2].2H_2O$ which showed rather very-good colour-fastness for the nylon in soapy H_2O. The possible reason for this on the nylon fabric was the synthetic nature of nylon fabric, the hydrophobicity of the synthetic fiber; the compact, crystalline structure, hindering dye penetration of the synthetic fiber; and the relatively low absorbency of the synthetic fiber. Nylon's synthetic nature and hydrophobic properties make it more resistant to dye adsorption. It is also worthy of note that cotton, being a natural hydrophilic fiber with an open cellulose structure, absorbs dye most easily (Yu et al., 2018; Gürbüz, 2020).

Corrosion Inhibition Results

Table 5 below denotes that change in weight (Δw), and consequent corrosion rate was highest for the blank in all cases, with a higher blank value for 373 K temperature when compared to that of 303 K temperature. This sets off the confirmation that the imine ligand and their complexes possess potency for corrosion inhibition on the mild steel surface, and that the rate of corrosion is a direct function of temperature (Festus et al., 2023), as demonstrated in figure 1.

Figure 1 shows the graphical corrosion studies relationship between corrosion rate (calculated from the weight loss values) of the mild steel, and concentrations of the imine ligands and their heteroleptic M(II) complexes, conducted in 1 M HCl acid solution, at constant temperature of 303K after 4 h. Ligand L2H at 303K after 4 h gave corrosion rate values of 0/001781 at 15 ppm, 0/001038 at 30 ppm and 0.0005 266 at 60 ppm.

A progressive decrease in the rate of corrosion as the concentration of the ligand increased from 15 ppm to 60 ppm was observed. The latter was a result of progressive decrease in the weight loss values against concentration values. The corrosion values of L2H were sharply different from the corrosion rate of the blank at 303K (0.002 345). Similar trends were observed for L1H. For and the metal complexes.

As observed in all the synthesized compounds, the relationship between corrosion rate and concentration were the same. That's corrosion rate was inversely proportional to the concentration of the imine compounds which agrees with the findings of Festus et al., (2023). The decrease in corrosion rate with increase in inhibitor concentration could be probably due to more effective adsorption of the compounds onto the mild steel surface since more molecules of the compounds were available in the 1 M HCl solution as the concentration increased (Jyito & Kumar, 2019). The more molecules of the imine-based compounds present in the solution, the more adsorption, and this results in decrease in the corrosion rate in the acidic medium.

At 303K, L1H had the highest corrosion rate performance than L2H at 15 ppm, 30 ppm and 60 ppm. Copper complex had the highest corrosion rate performance over the three other metal complexes, at 15 ppm 30 ppm and at 60 ppm. However, the corrosion rate performance for L1H was less than that for copper. This corroborates findings in existing literature confirming that metal complexes are more effective corrosion inhibitors than their ligand precursors (Nnenna et al., 2020, N'guessan et al., 2021).

Figure 2 shows the graphical relationship between corrosion rate and concentration carried out after 4 h of immersion in 1 M HCl solution at varied concentrations of 373K temperature. Separately, a progressive fall in the corrosion rates of the ligands as concentration increased were observed. However, L1H showed higher corrosion rate performance than L2H suggesting that at 373K, L1H was more corrosion inhibitive than L2H.

Comparing the corrosion rate performances of the compounds at 303K and 373K, a reduction at 373K was noticed. This result confirmed that corrosion rate was affected by temperature (Madueke & Iroha, 2018). The copper complex had the least corrosion rate value (highest corrosion rate performance) at 303K, making the compound the most effective corrosion inhibitor amongst all the compounds at 303K. Though, the iron complex showed the highest corrosion rate performance at 373K.

Figure 3 shows the graphical relationship between the surface coverage of the mild steel coupons by the different concentrations in 1 M HCl acid solution environment. The surface coverage was calculated based on the corrosion rate in the absence and presence of the compounds. Hence, the trends observed in the corrosion reports for the imines given were expected to be similar in all aspects. Each showed the increase in surface coverage as the concentration of the ligands increased from 15-30 ppm. The surface coverage was directly proportional to the concentration. This was in concordance to Madueke & Iroha (2018) in their research on corrosion inhibition studies.

Cite this article as:
Iyo, I.A., Festus, C., &Amadi, J.U. (2025). Corrosion inhibition and dye studies of mixed-ligand metal (II) complexes: synthesis and characterization. *FNAS Journal of Scientific Innovations*, *6*(3), 15-27. https://doi.org/10.63561/fnas-jsi.v6i3.946

Figure 4 shows a graphical relationship between surface coverage and concentration at 373K after 4 h duration in a 1 M HCl acid medium. Surface coverage results for L2H were 0.1168 (15 ppm), 0.6878 (30 ppm) and 0.7168 (60 ppm); and for L1H were 0.2897 (15 ppm), 0.4397 (30 ppm) and 0.5611 (60 ppm). The progressive rise in the values of surface coverage as the concentration increased could be due to linear relationship between surface coverage and concentration as more molecules of the compounds were present in solution at higher concentrations.
However, in comparing the surface coverage results of the ligands and their heteroleptic M(II) compounds at 303K and 373K, a significant fall in surface coverage ability for all the compounds at 373K was observed. The inverse relationship between surface coverage and temperature owes to the weakness of the adsorption strength of the imines onto the mild steel surface as a result of increase in the kinetics of the system but decrease in the equilibrium constant (Madueke & Iroha, 2018). This summarized those higher temperatures results in a decrease in the values of surface coverage (Festus et al., 2023).
Figure 4, L1H had a higher surface coverage than L2H at 15 ppm, but L2H had a higher surface coverage than L1H at 60 ppm. At 15 ppm and 60 ppm, Fe(II) complex had the highest surface coverage than all other complexes.

Figure 5 shows a graphical representation of the results obtained at 303K with respect to corrosion inhibition efficiency and concentration in 1M HCl acid solution wherein mild steel coupons were immersed for 4h. Assessing the ligands L2H and L1H, a general rise in corrosion inhibition efficiency as the concentration of the substances respectively increased from 15 ppm to 60 ppm was observed.
Comparing the corrosion inhibition efficiency of the ligands and their heteroleptic M(II) complexes at 303K after 4 hours of immersion, performances favoring the M(II) complexes were noticed. L1H had a better performance than Zn(II) and Fe(II) complexes at 15 ppm, but the M(II) complexes outperformed the ligand L1H at 30 ppm and 60 ppm, except for the Zn(II) complex which had a lower efficiency than L1H at 30 ppm. The better corrosion inhibition efficiency of the M(II) complexes over the ligands from which they were made was expected following coordination traces on the mild steel by the M(II) ions, the nitrogen, oxygen and the sulfur atoms within the heteroleptic M(II) complexes (bearing also in mind that complexes having sulfur donor atom are better coordinative and adsorbing species) (N'guessan et al., 2020).

Figure 6 shows the variation between the corrosion inhibition efficiency on mild steel in 1 M HCl acid solution and the concentration of the compounds at 373K after 4 h. There was some observable difference in the height of the bars of the chart at 373K when compared with the bar chart at 303K.

At 15 ppm, L1H performed better in inhibition efficiency than L2H; while at 30 ppm and 60 ppm L2H had a better performance than 2L8A, which gives L2H a better option in inhibiting corrosion of mild steel on the average. Comparing the corrosion inhibition efficiency performance of the ligands at 303 K and 373K there is a fall at 373K, indicating that corrosion inhibition efficiency is affected by temperature: the corrosion inhibition efficiency reduces as the temperature increases (Madueke & Iroha, 2018). The lower corrosion inhibition efficiency performance reduction at higher temperature can be attributed to the desorption that occurs between the donor atoms and the surface of the mild steel due to increase in the kinetics and decrease in the thermodynamic equilibrium of the system (Madueke & Iroha, 2018).

In summary of the corrosion studies results, on average, L1H had better corrosion inhibition efficiency at 303K, while L2H had better results at 373 K. Cu(II) complex had highest corrosion inhibition efficiency results on average, at 303 K, followed by Fe(II) and Ni(II) complexes; while at 373K the Fe(II) complex showed highest corrosion inhibition efficiency, followed by Ni(II) and Cu(II) complexes.

Conclusion

The corrosion rate in the absence of the inhibitors increased more than it that in the presence of the inhibitor at constant temperature, suggestive that the imine ligands and their M(II) complexes are good corrosion inhibitors in acid milieu. The corrosion rate was lower at lower temperature both in the absence and presence of the Schiff- base compounds, confirming that corrosion rate is directly proportional to temperature.The corrosion rate values in the presence of the inhibitors decreased as the concentration of the inhibitor increased, suggestive that the imine compounds are significant in corrosion inhibition.Surface coverage values were higher at lower temperature and higher concentrations for the imine compounds, confirming the adsorption of the imine compounds onto the surface of the mild steel immersed in the acid. This also confirms the inverse relationship, and direct relationship, between surface coverage and temperature, and concentration, respectively. Corrosion inhibition efficiency values were higher at lower temperature and higher concentrations for the imine compounds, confirming the efficacy of the imine compounds as

Cite this article as:
Iyo, I.A., Festus, C., &Amadi, J.U. (2025). Corrosion inhibition and dye studies of mixed-ligand metal (II) complexes: synthesis and characterization. *FNAS Journal of Scientific Innovations*, *6*(3), 15-27. https://doi.org/10.63561/fnas-jsi.v6i3.946

good corrosion inhibitors for the mild steel immersed in the acid. This also confirms the inverse relationship, and direct relationship, between corrosion inhibition efficiency and temperature, and concentration, respectively. The imine ligands and their M(II) complexes showed significant result on the SBS with ranges 4–5 on both natural and synthetic fabrics when agitated in both soapy and non-soapy H_2O at temperature slightly above room temperature and in considerable amount of time. This good-to-excellent result (4–5) produced by these azo dyes is suggestive of the viable potency of these compounds to be employed as possible dye alternative on both cellulose and non-cellulose fabrics.For their ease of biodegradability and relatively non-toxic and cost-effective nature these imine dyes are recommended to textile industries as viable dyestuff alternative on textile fabrics

References

Abel-Olaka, L. C., Kpee, F., & Festus, C. (2019). Solvent extraction of 3*d* metallic elements using N_2O_2 Schiff base-chelators: Synthesis and characterization. *Nigerian Research Journal of Chemical Sciences, 7*(2), 133-146.

Abdel-Rahman, L. H., El-Khatib, R. M., Abdel-Fatah, S. M., Moustafa, H., Alsalme, A. M., & Nafady, A. (2019). Novel Cr (III), Fe (III) and Ru (III) Vanillin based metallo pharmaceuticals for cancer and inflammation treatment: experimental and theoretical studies. *Application of Organometallic Chemistry 33*, 5177.

Abdel-Rahman, L. H., Ismail, N. M., Ismael, M., Abu-Dief, A. M., & Ahmed, E. A. (2017). Synthesis, characterization, DFT calculations and biological studies of Mn(II), Fe(II), Co(II) and Cd(II) complexes based on a tetradentate ONNO donor Schiff base ligand. *Journal of Molecular Structure, 1134*, 851-862.

Abou-Hussein, A. A. & Linert, W. (2014.) Synthesis, spectroscopic, coordination and biological activities of some organometallic complexes derived from thio-Schiff base ligands. *Spectrochim Acta-Part A Mol Biomol Spectrosc,. 117*.

Abuamer, K. M., Maihub, A. A., El-Ajaily, M. M., Etorki, A. M. (2014), Abou-Krisha, M. M. & Almagani, M. A. (2014). The Role of Aromatic Schiff Bases in the Dyes Techniques. *International Journal of Organic Chemistry, 4*. http://dx.doi.org/10.4236/ijoc.2014.41002.

Abuamer, K. M., Maihub, A. A., El-Ajaily, M. M., Etorki, A. M., Abou-Krisha, M. M. & Almagani, M. A. (2014). The role of aromatic Schiff bases in the dyes techniques. *International Journal of Organic Chemistry, 4*, 7-15. Http://dx.doi.org/10.4236/ijoc.2014.41002.

Aburas, N. M., Stevanovic, N. R. & Milcic, M. K. (2013). Influence of the structure on the antioxidant activity of tetradentate Schiff bases and their copper(II) complexes. *Possible Mechanisms. Journal of the Brazilian Chemical Society, 24*, 1322. https://doi.org/10.5935/0103-5053.20130167.

Alam, M. S., Lee, D. U. & Bari, M. L. (2014). Antibacterial and cytotoxic activities of Schiff base analogues of 4-aminoantipyrine. *Journal of the Korean Society for Applied Biological Chemistry, 57*, 613-619. https://doi.org/10.1007/s13765-014-4201-2.

Aliyu, H. N. & Sani, U. (2012). Synthesis, characterization and biological activity of Mn(II), Fe(II), Co(II), Ni(II), and Co(II). Schiff base chelates against multidrug resistant bacteria and fungi pathogens. *International Research Journal of pharmacy and Pharmacology, 2*, 40 – 44

Chioma, F., Chizoba, I. E. & Obinna, O. (2023). Synthesis, characterization, DFT and biological studies of Fe(II), Cu(II), and Zn(II) complexes of keto-imine chelators. *Inorganica Chimica Acta*, 545. https://doi.org/121255.

Chioma, F., Ima-Bright, N., & Osi, V. (2022). Synthesis, spectral, computational studies and antimicrobial evaluations of Fe(II) and Zn(I) chelates containing RC-NR and N_2O_2 moieties. *Journal Analytical Pharmaceutical Research, 1*(2), 45-54. https://doi.org/10.15406/japlr.2022.11.00401.

El-Ajaily, M., Maihub, A., Etorki, A., Ben-Saber, S. & Elmajani, M. (2013). Coordination behavior of phenolic and benzylic hydroxyl groups in complexation of their Schiff bases with Zn(II) and Cd(II) ions. *Journal of Pharmaceutical and Biomedical Sciences, 8*, 695-697.

Festus, C. & Okocha, O. (2017). Behaviour of N-(2- hydroxybenzylidene)pyrazine-2-carboxamide in complexation towards Fe(II), Co(II), Ni(II) and Cu(II) ions: synthesis, spectral characterization, magnetic and antimicrobial properties. *International Journal of Chemistry, Pharmaceuticals &Technology, 2*(4); 143-153.

Festus, C., & Wodi, C. T. (2021). Corrosion inhibition; and antimicrobial studies of bivalent complexes of 1-(((5-ethoxybenzo[d]thiazol-2-yl)Imino)methyl)naphthalene-2-ol chelator: design, synthesis, and experimental characterizations. *Direct Research Journal of Chemistry and Materials Science, 8*(2021); 31-43.

Festus, C., Odozi, W. N., Mchihim, M. M., & Olatunde, M. A. (2022). Synthesis, spectroscopic, density functional theory and corrosion inhibitive studies of *N*-(1,4-dihydro-1,4-dioxonapthalene-3-yl)pyrazine-2-carboxamide chelator-ligand. *Global Journal of Pure and Applied Sciences, 28*, 39-50.

Festus, C., Obinna O., Sunday N. O., & Ezugwu, C. I. (2023). Antimicrobial, antioxidant, and insilco studies of divalent metal complexes of novel aminopyrimidine Schiff base chelators. *Journal of Molecular Structure, 1291*(2023), 1-12.

Festus, C., Wodi, T. C. & Iyo, I. A. (2023). Performance of organic frameworks as thriving mild steel corrosion inhibitors in acid medium: syntheses and characterization. *Protection of Metals and Physical Chemistry of Surfaces*. https://doi.org/10.1134/S2070205123700594

Gupta, M., He, J., Nguyen, T., Petzold, F., Fonseca, D., Jasinski, J., Sunkara, M. (2016). Nanowire catalysts for ultra-deep hydro-desulfurization and aromatic hydrogenation. *Applied Catalysis B: Environmental*, *180*, 246-254. https://doi.org/10.1016/j.apcatb.2015.06.029.

Gürbüz, D. (2020). Dyeing polyester, cotton and wool with some Schiff bases derived from 4- chloroaminophenol and various benzaldehydes. *JOTCSA, 7*(2), 463-70.

Jane, A. & Chioma F.(2024). Antimicrobial and corrosion inhibition studies of homoleptic metal (II) complexes of fluoroaniline schiffbase: Synthesis and characterization. *Scientific Modelling and Research,* 9(1), 69-88.

Jyito, D. & Kumar, H. (2019). Synthesis, characterization and application of Schiff base metal complexes. *Journal of Emerging Technologies and Innovative Research 6*(5). https://www.jetir.org.

Kpee, F., Ukachukwu, C. V. & Festus, C. (2018). Synthesis, characterization and extractive potentials of aminopyrimidine Schiff base ligands on divalent metal ions. *Nigerian research journal of chemical sciences, 4*(2), 193-203.

Kumar, N., Pratima, S., Aastha, P. & Prasad, A. (2013). Synthesis and characterization of some new shiff bases. *International Journal of Chemical and Pharmaceutical Sciences, 23*(2), 231-236. https://doi.org/10.3390/ijms151120800.

Kumar, N., Pratima, S., Aastha, P. & Prasad, A. V. G. S. (2013). Synthesis and characterization of some new Schiff bases. *International Journal of Chemical and Pharmaceutical Sciences, 23*(2), 231-236.

Le Goff, G. & Ouazzani, J. (2014). Natural hydrazine-containing compounds: biosynthesis, isolation, biological activities and synthesis. *Bioorganic & Medicinal Chemistry, 22*(23), 6529-6544, https://doi.org/10.1016/j.bmc.2014.10.011.

Madueke, N. A. & Iroha, N. B. (2018). Protecting aluminium alloy of type AA8011 from acid corrosion using extract from allamanda cathartica leaves. *International Journal of Innovative Research in Science, Engineering and Technology, 7*(10). https://doi.org/10251.

Memon, S. Q., Memon, N., Mallah, A., Soomro, R. & Khuhawar, M. Y. (2014). Schiff bases as chelating reagents for metal ions analysis. *Current Analytical Chemistry. 10*, 393-417.

Mohanraj, M, Ganesan, A., Raja, G. & Jayabalakrishnan, C. (2016). Evaluation of DNA binding, DNA cleavage, protein binding, radical scavenging and *in vitro* cytotoxic activities of ruthenium(II) complexes containing 2,4-dihydroxy benzylidene ligands. *Materials Science and Engineering, 69*, 1297-1306. https://doi.org/10.1016/j.msec.2016.08.043.

N'guessan, Y. S. D., Nagnonta, H. C., Ollo, K. & Albert, T. (2021). Experimental and theoretical investigations on copper corrosion inhibition by cefixime drug in 1 M HNO_3 solution. *Journal of Materials and Chemical Engineering, 9*, 11-28. Https://www.scirp.org/journal/msce.

Nair, S., Arish, D. & Joseyphus, R. S. (2014.)Synthesis, characterization, antifungal, antibacterial and DNA cleavage studies of some heterocyclic Schiff base metal complexes. *Journal of Saudi Chemical Society, 16*(1), 83–88.

Nnenna, W. O., Festus, C. & Muhammed, A. D. (2020). Synthesis, adsorption and inhibition behaviour of 2(thiophen-2-ylmethylidene) aminespyridine -3-olon mild steel corrosion in aggressive acidic media. *Nigerian Research Journal of Chemical Sciences. 8*(2); 291-307. Http://www.unn.edu.ng/nigerian-researchjournal-of-chemical-sciences/ 291.

Osowole, A. A. & Festus, C. (2013). Synthesis, characterization and antibacterial activities of some metal(II) complexes. *Elixir Application Chemistry, 59*, 15843–15847. https://doi.org/10.9734/IRJPAC/2014/1540.

Sani, U. 1. & Iliyasu, S. (2018). Synthesis, characterization and antimicrobial studies on Schiff base derived from 2-aminopyridine and 2-methoxybenzaldehyde and its cobalt(II) and nickel(II) complexes. *Bayero Journal of Pure and Applied Sciences 11*(1), 214 – 219. http://dx.doi.org/10.4314/bajopas.v11i1.355.

Yang, Y., Gao, C. Y. & Liu, J. D. (2016). Recent developments in rhodamine salicylidene hydrazone chemosensors. *Analytical Methods*, ***8***, 2863-2871. https://doi.org/10.1039/C6AY00135A.

Yu, F., Wang, Z., Zhang, S., Ye, H., Kong, K., Gong, X., Hua, J. & Tian, H. (2018). Molecular engineering of donor-acceptor conjugated polymer/g- C3N44 heterostructures for significantly enhanced hydrogen evolution under visible- light irradiation. *Advanced Functional Materials,, 28*. https://doi.org/1804512.

Cite this article as:
Iyo, I.A., Festus, C., &Amadi, J.U. (2025). Corrosion inhibition and dye studies of mixed-ligand metal (II) complexes: synthesis and characterization. *FNAS Journal of Scientific Innovations*, *6*(3), 15-27. https://doi.org/10.63561/fnas-jsi.v6i3.946